OMTM, Volume *32*

Supplemental information

Glycosylation of recombinant adeno-associated virus serotype 6

Yuki Yamaguchi, Kentaro Ishii, Sachiko Koizumi, Hiroaki Sakaue, Takahiro Maruno, Mitsuko Fukuhara, Risa Shibuya, Yasuo Tsunaka, Aoba Matsushita, Karin Bandoh, Tetsuo Torisu, Chie Murata-Kishimoto, Azusa Tomioka, Saho Mizukado, Hiroyuki Kaji, Yuji Kashiwakura, Tsukasa Ohmori, Atsushi Kuno, and Susumu Uchiyama

Table S1. Sample information of the lectin microarrays used for the PCA analysis shown in Figure 1B. The number and color correspond to the dot in PCA score plot.

The dot number	Sample	Amount (vg)
1	Sample 1	2.5×10^{9}
2	Sample 1	1×10^{10}
3	Sample 1	4×10^{10}
4	Sample 2	2.5×10^{9}
5	Sample 2	1×10^{10}
6	Sample 2	4×10^{10}
7	Sample 3	2.5×10^{9}
8	Sample 3	1×10^{10}
9	Sample 3	4×10^{10}
10	Sample 3	2.5×10^{9}
11	Sample 4	2.5×10^{9}
12	Sample 4	1×10^{10}
13	Sample 4	4×10^{10}
14	Sample 5	2.5×10^{9}
15	Sample 5	1×10^{10}
16	Sample 5	4×10^{10}
17	Sample 6	2.5×10^{9}
18	Sample 6	5×10^{9}

Table S2. The list of identified proteins contaminating Sample 4.

Several bovine serum proteins (colored blue) and human galectin 3-binding protein (colored red) were identified in Sample 4.

Accession	-10lgP	Coverage (%)	Area	#Peptides	Avg. Mass	Description
VP1_AAV6	215.39	74	3.81E+08	47	81411	VP1_AAV6
#CONTAM#Q7SIH1|A2MG_BOVIN	241.3	66	3.35E+08	77	167575	Alpha-2-macroglobulin OS=Bos taurus OX=9913 GN=A2M PE=1 SV=2
#CONTAM#A7E3W2|LG3BP_BOVIN	174.09	40	6.08E+07	18	62127	Galectin-3-binding protein OS=Bos taurus OX=9913 GN=LGALS3BP PE=1 SV=1
#CONTAM#Q3Y5Z3|ADIPO_BOVIN	115.09	32	2.42E+07	6	26133	Adiponectin OS=Bos taurus OX=9913 GN=ADIPOQ PE=1 SV=1
#CONTAM#P06748|NPM_HUMAN	147.68	46	2.23E+07	10	32575	Nucleophosmin OS=Homo sapiens OX=9606 GN=NPM1 PE=1 SV=2
#CONTAM#O46415|FRIL_BOVIN	129.49	63	2.01E+07	10	19988	Ferritin light chain OS=Bos taurus OX=9913 GN=FTL PE=2 SV=3
#CONTAM#P02792|FRIL_HUMAN	122.99	48	1.52E+07	9	20020	Ferritin light chain OS=Homo sapiens OX=9606 GN=FTL PE=1 SV=2
#CONTAM#P55072|TERA_HUMAN	199	68	8.51E+06	47	89322	Transitional endoplasmic reticulum ATPase OS=Homo sapiens OX=9606 GN=VCP PE=1 SV=4
#CONTAM#Q01853|TERA_MOUSE	199	68	8.51E+06	47	89322	Transitional endoplasmic reticulum ATPase OS=Mus musculus OX=10090 GN=Vcp PE=1 SV=4
#CONTAM#P46462|TERA_RAT	199	68	8.51E+06	47	89349	Transitional endoplasmic reticulum ATPase OS=Rattus norvegicus OX=10116 GN=Vcp PE=1 SV=3
#CONTAM#P00761|TRYP_PIG	93.86	34	6.47E+06	5	24409	Trypsin OS=Sus scrofa OX=9823 PE=1 SV=1
#CONTAM#P04406|G3P_HUMAN	153.88	58	5.76E+06	17	36053	Glyceraldehyde-3-phosphate dehydrogenase OS=Homo sapiens OX=9606 GN=GAPDH PE=1 SV=3

#CONTAM#Q5R8J7|FRIH_PONAB	138.85	72	5.65E+06	13	21226	Ferritin heavy chain OS=Pongo abelii OX=9601 GN=FTH1 PE=2 SV=3
#CONTAM#P02794|FRIH_HUMAN	138.85	72	5.65E+06	13	21226	Ferritin heavy chain OS=Homo sapiens OX=9606 GN=FTH1 PE=1 SV=2
#CONTAM#P14618|KPYM_HUMAN	168.02	53	5.50E+06	22	57937	Pyruvate kinase PKM OS=Homo sapiens OX=9606 GN=PKM PE=1 SV=4
#CONTAM#Q01105|SET_HUMAN	117.82	31	5.11E+06	9	33489	Protein SET OS=Homo sapiens OX=9606 GN=SET PE=1 SV=3
#CONTAM#Q9BXJ4|C1QT3_HUMAN	100.58	21	4.95E+06	5	26994	Complement C1q tumor necrosis factor-related protein 3 OS=Homo sapiens OX=9606 GN=C1QTNF3 PE=1 SV=1
#CONTAM#Q9BQA1|MEP50_HUMAN	145.04	43	4.67E+06	11	36724	Methylosome protein 50 OS=Homo sapiens OX=9606 GN=WDR77 PE=1 SV=1
#CONTAM#Q07021|C1QBP_HUMAN	118.24	41	4.42E+06	7	31362	Complement component 1 Q subcomponent-binding protein mitochondrial OS=Homo sapiens OX=9606 GN=C1QBP PE=1 SV=1
#CONTAM#P04075|ALDOA_HUMAN	163.86	73	4.41E+06	22	39420	Fructose-bisphosphate aldolase A OS=Homo sapiens OX=9606 GN=ALDOA PE=1 SV=2
#CONTAM#P02769|ALBU_BOVIN	178.52	58	3.64E+06	32	69294	Albumin OS=Bos taurus OX=9913 GN=ALB PE=1 SV=4
#CONTAM#P15636|API_ACHLY	132.47	16	3.33E+06	9	68125	Protease 1 OS=Achromobacter lyticus OX=224 PE=1 SV=1
#CONTAM#Q08380|LG3BP_HUMAN	139.96	29	2.95E+06	14	65331	Galectin-3-binding protein OS=Homo sapiens OX=9606 GN=LGALS3BP PE=1 SV=1
#CONTAM#P30048|PRDX3_HUMAN	108.06	31	2.82E+06	7	27693	Thioredoxin-dependent peroxide reductase mitochondrial OS=Homo sapiens OX=9606 GN=PRDX3 PE=1 SV=3
#CONTAM#Q5REY3|PRDX3_PONAB	108.06	31	2.82E+06	7	27700	Thioredoxin-dependent peroxide reductase mitochondrial OS=Pongo abelii OX=9601 GN=PRDX3 PE=2 SV=1

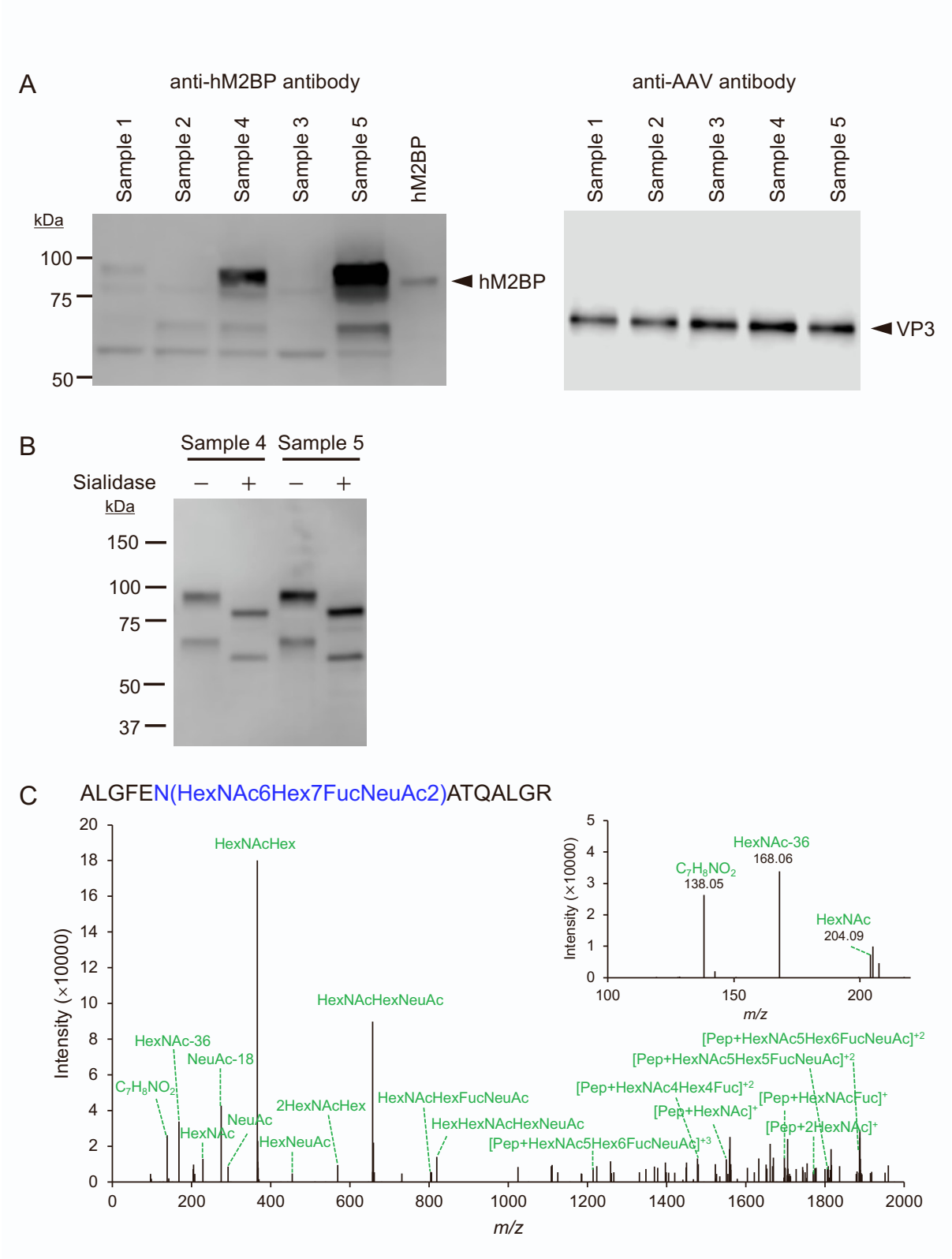

Figure S1. (A) Western blots of Samples 1–5 detected with anti-hM2BP antibody (left) and anti-AAV viral proteins antibody (right). (B) Western blot analysis of Samples 4 and 5 detected with anti-hM2BP antibody with and without sialidase treatment. (C) The CID mass spectra of hM2BP A64–R76 modified with HexNAc6Hex7FucNeuAc2 in Sample 4.

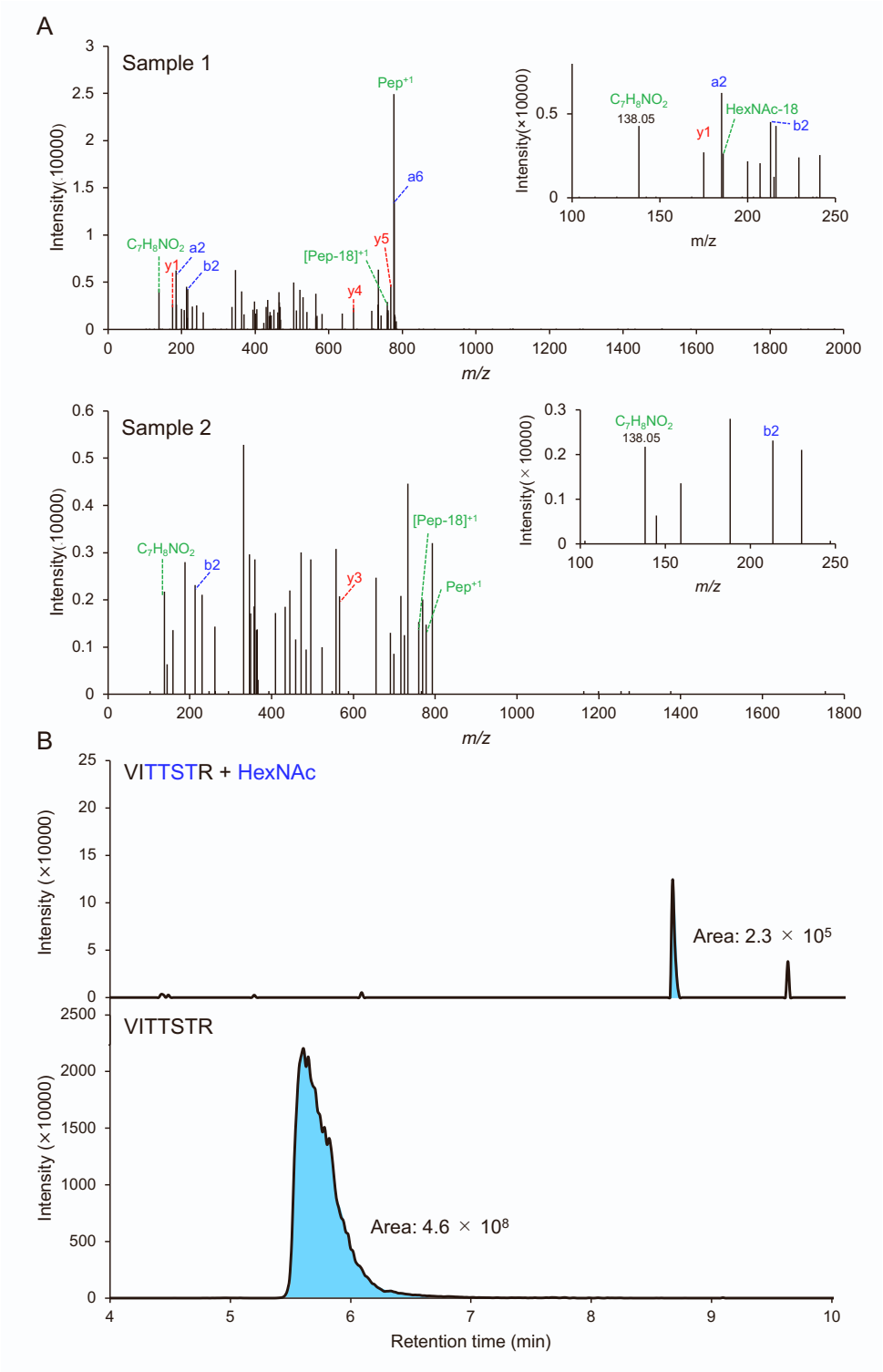

Figure S2. (A) The CID mass spectra of V239–R245 modified with HexNAc for Samples 1 and 2. (B) Extracted ion chromatograms (XICs) of V239–R245 modified with HexNAc (*m/z* 389.2284) (top) and unmodified V239–R245 (*m/z* 490.7697) (bottom). Each MS area was calculated using Byos software. The amount of peptide modified with *O*-GlcNAc (*a*) was calculated with the equation: a = [2.3 × 10^5 of *O*-GlcNAc modified peptide's MS area] / ([*O*-GlcNAc modified peptide's MS area] + [4.6 × 10^8 of unmodified peptide's MS area]). The percentage of particle modified with *O*-GlcNAc (p) was calculated with the equation: $p = 1^{60} – (1\text{-}0.0005)^{60}$.

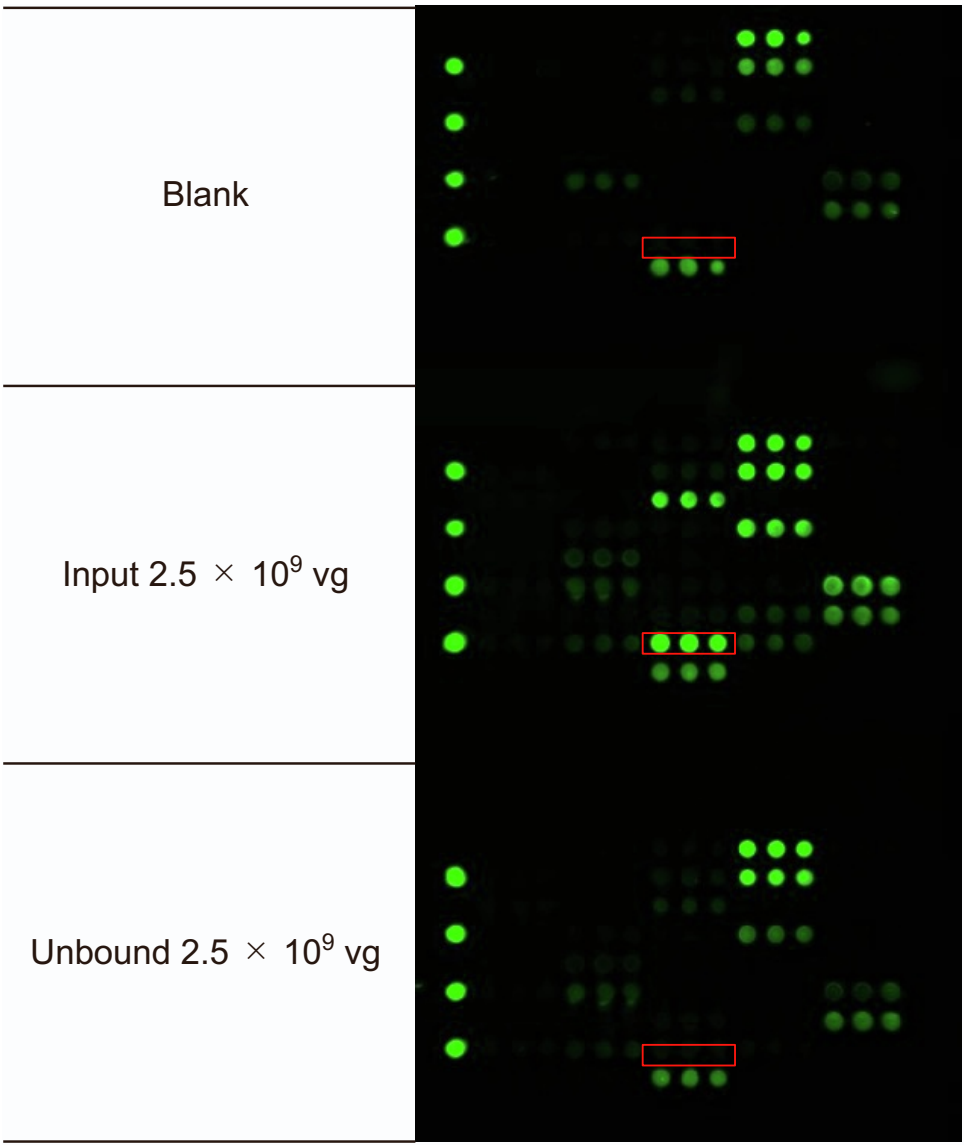

Figure S3. The signals detected by lectin microarray for 2.5 × 10^9 vg rAAV6 samples as described for western blotting. The area of ABA signals is marked by in a red box. The Blank array shows the high signals of *Lycopersicon esculentum* lectin (LEL), *Solanum tuberosum* lectin (STL), and *Urtica dioica* lectin (UDA) in triplicate spots caused by binding to the detection antibody. The signals of those lectins were therefore excluded from the lectin microarray analysis.

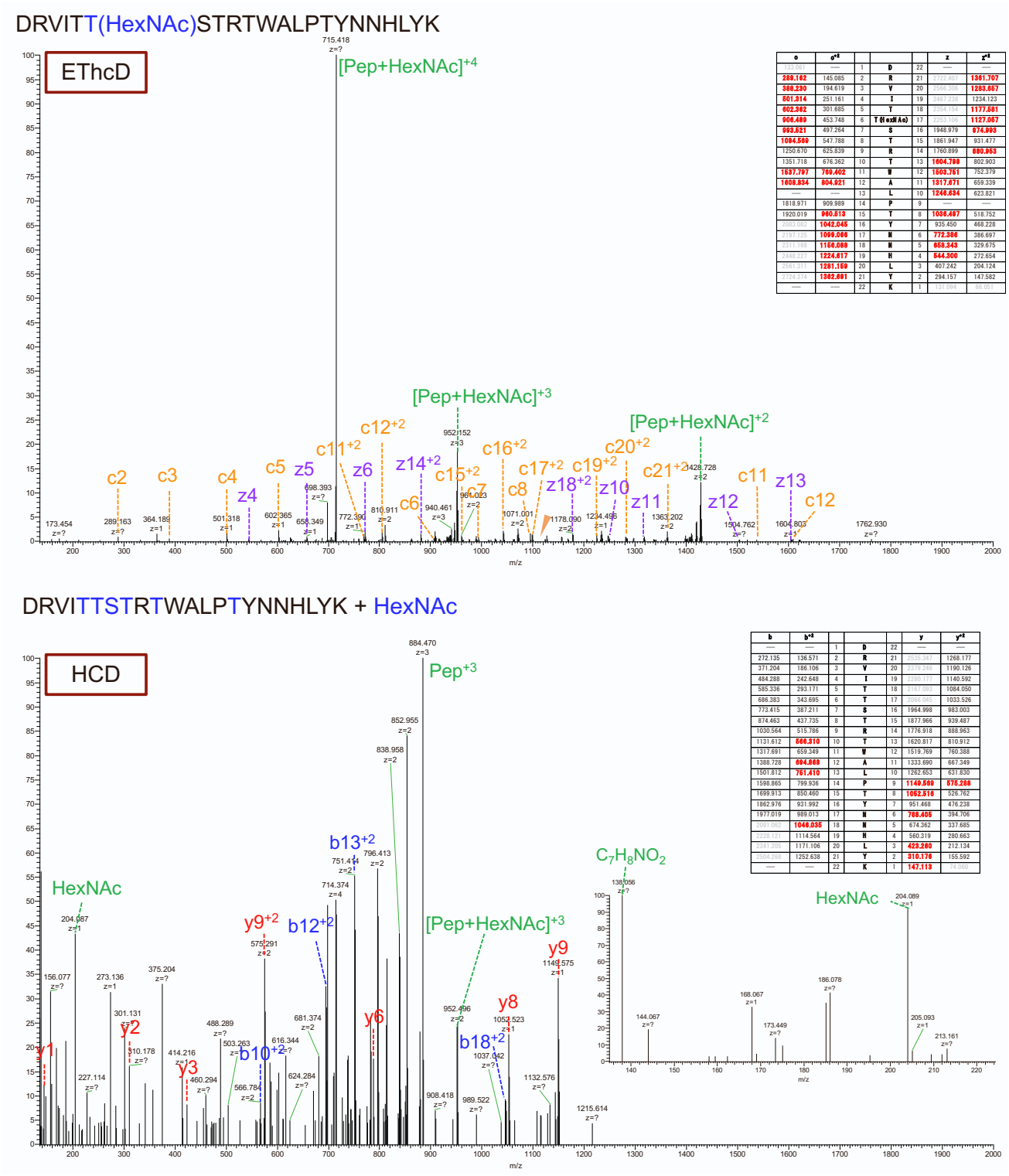

Figure S4. The EThcD and HCD mass spectra of D237–K258 with HexNAc identified in the unbound fraction of rAAV6.

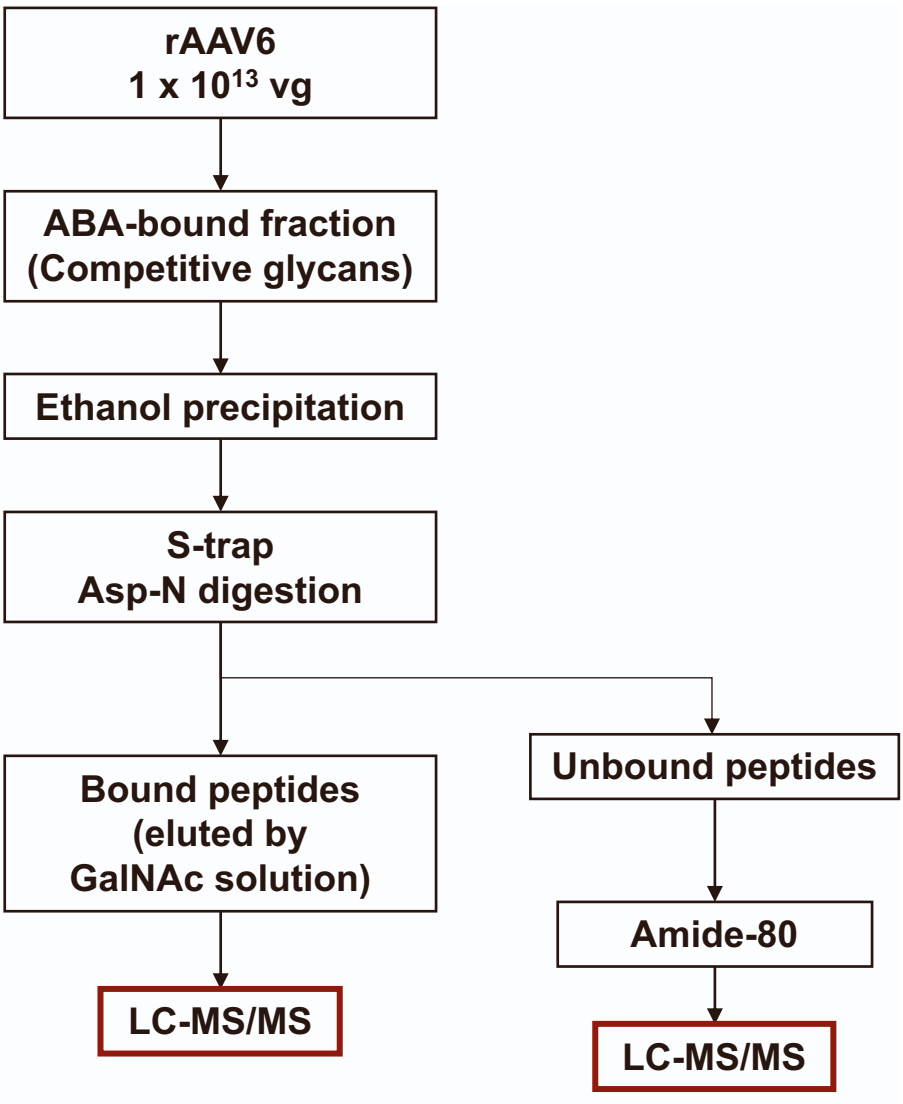

Figure S5. The experimental workflow of LC-MS/MS analysis for the bound fraction of rAAV6 using Sample 1.

A

O-glycan							
DSSSGIGKTGQQPAKKRLNFGQTG (154–177)							
cluster_no:1/member:3							
peak_no	m/z	rt	intensity	Hex	HexNAc	dHex	NeuAc
1	2462.268	40.99	158184080	0	0	0	0
570	2665.354	40.79	184328	0	1	0	0
217	2665.354	39.99	639783				
878	2868.434	39.59	98248	0	2	0	0

O-glycan							
DPQPLGEPPATPAAVGPTTM (ox)ASGGGAPM (ox)A (184–212)							
cluster_no:5/member:10							
peak_no	m/z	rt	intensity	Hex	HexNAc	dHex	NeuAc
497	2881.321	61.9	302018	0	1	0	0
346	3043.372	61.06	572997	1	1	0	0
1985	3043.376	62.69	21129				
1102	3043.378	62.01	66605				
636	3084.399	60.83	191739	0	2	0	0
1970	3246.451	59.43	21498	1	2	0	0
879	3246.452	60.08	101782				
2698	3246.453	58.76	9019				
2361	3334.466	64.29	13970	1	1	0	1
596	3334.469	62.63	215796				
1677	3334.469	63.46	30550				
1041	3334.47	60.26	74799				
2550	3408.509	58.76	11121	2	2	0	0
2117	3537.548	60.35	18564	1	2	0	1
780	3537.549	61.58	123455				
1480	3537.549	59.21	38553				
282	3625.561	61.06	774921	1	1	0	2
1706	3625.563	63.29	29419				
1945	3625.566	64.73	22098				
431	3828.646	59.87	388762	1	2	0	2
1005	3845.674	59.87	81457	2	2	1	1

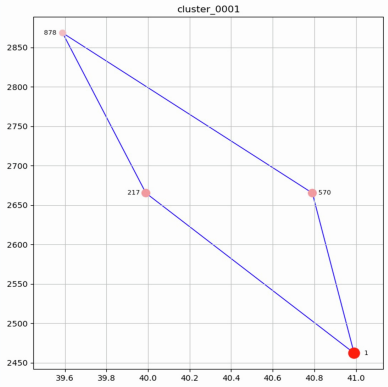

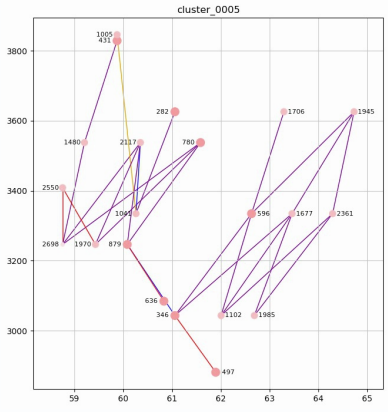

B DSSSGIGKTGQQPAKKRLNFGQTG

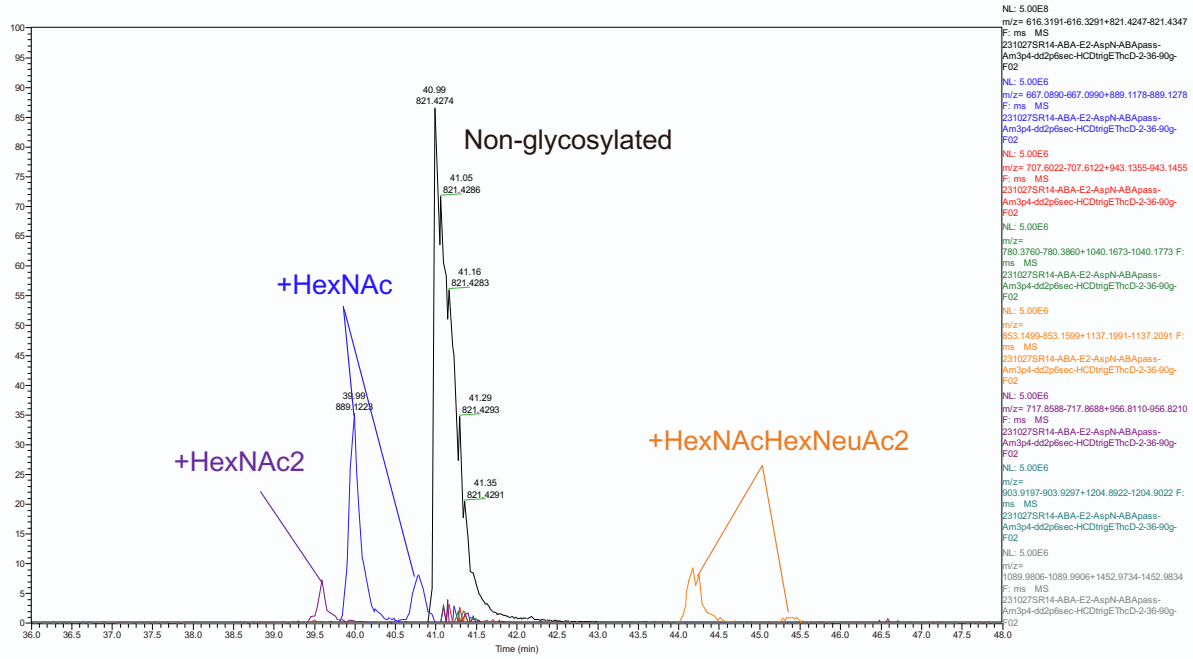

Figure S6. (A) Glycopeptide clusters assigned by GRable for D156–G177 and D184–A212 of the fractionated rAAV6. (B) XICs of D156–G177 modified with mucin-type *O*-glycan clusters. The signal of non-glycosylated peptide (*m/z* 821.4297 ± 0.005) is colored black, HexNAc (*m/z* 889.1228 ± 0.005) is blue, HexNAc2 (*m/z* 956.8160 ± 0.005) is purple and HexNAcHexNeuAc2 (*m/z* 1137.1941 ± 0.005) is orange.

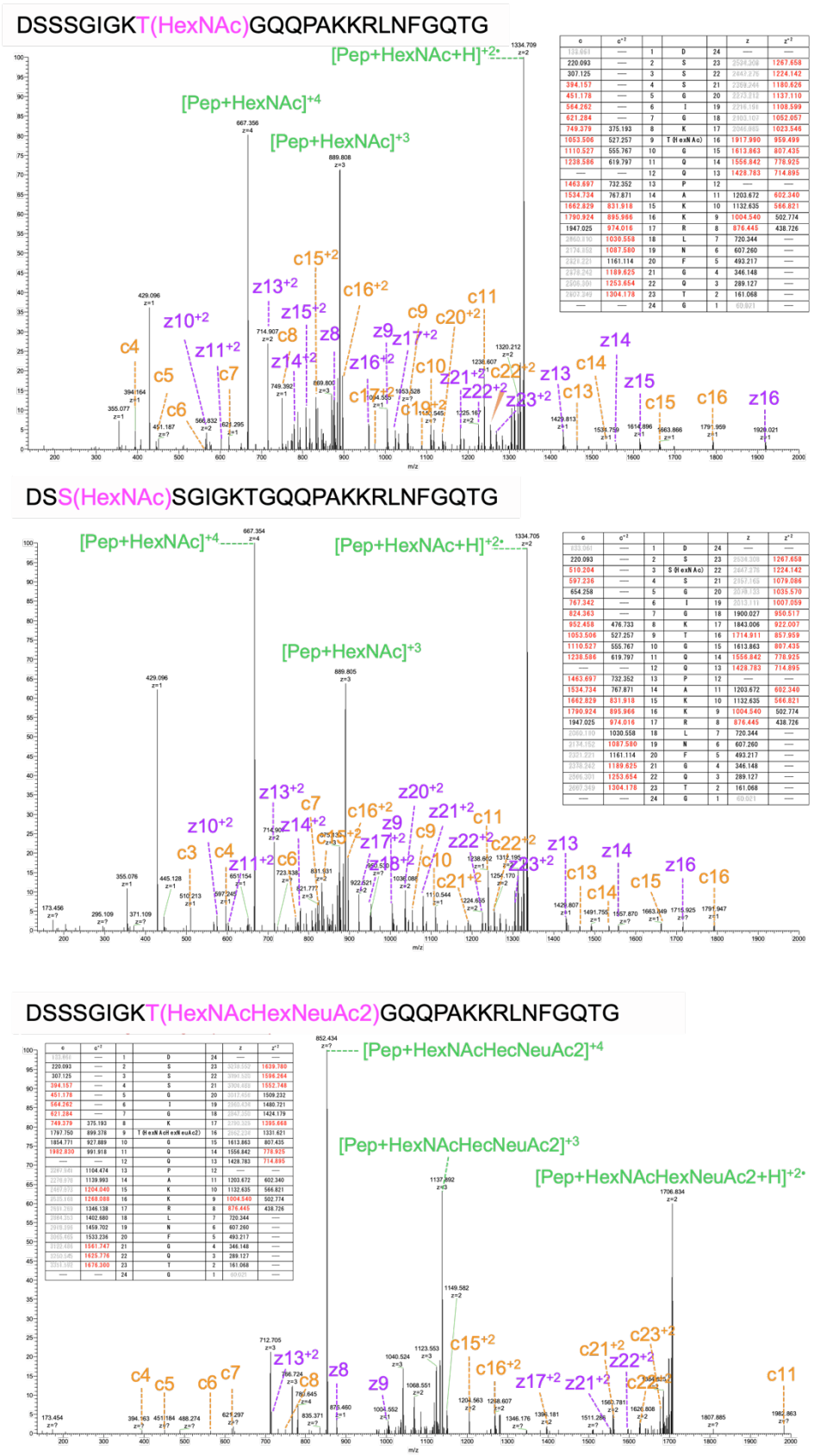

Figure S7. The EThcD mass spectra of D156–G177 modified with HexNAc at T162 (top), HexNAc at S156 (middle) and HexNAcHexNeuAc2 (bottom).

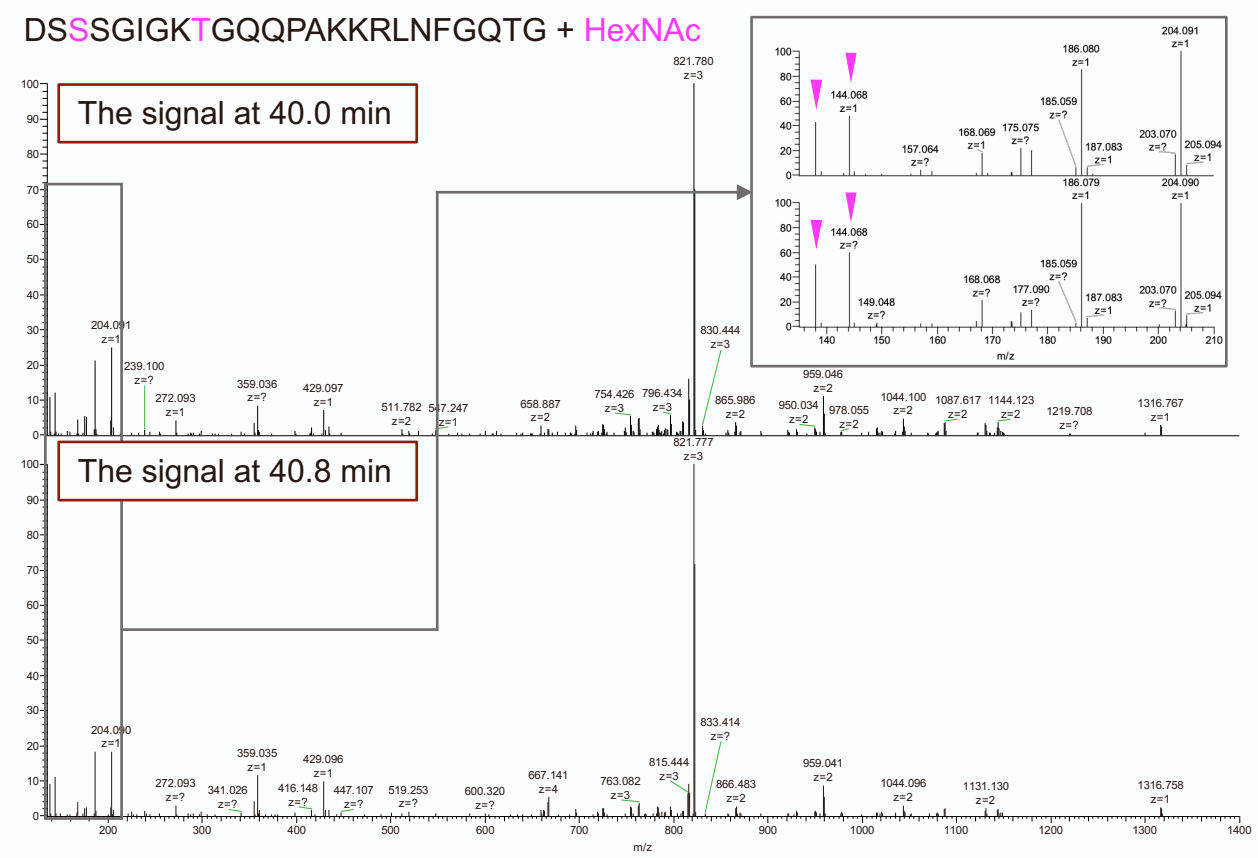

Figure S8. The HCD mass spectra of the signals at 40.0 min and 40.8min for D156–G177 modified with HexNAc. The signals *m/z* 138 and *m/z* 144 showed similar intensities.

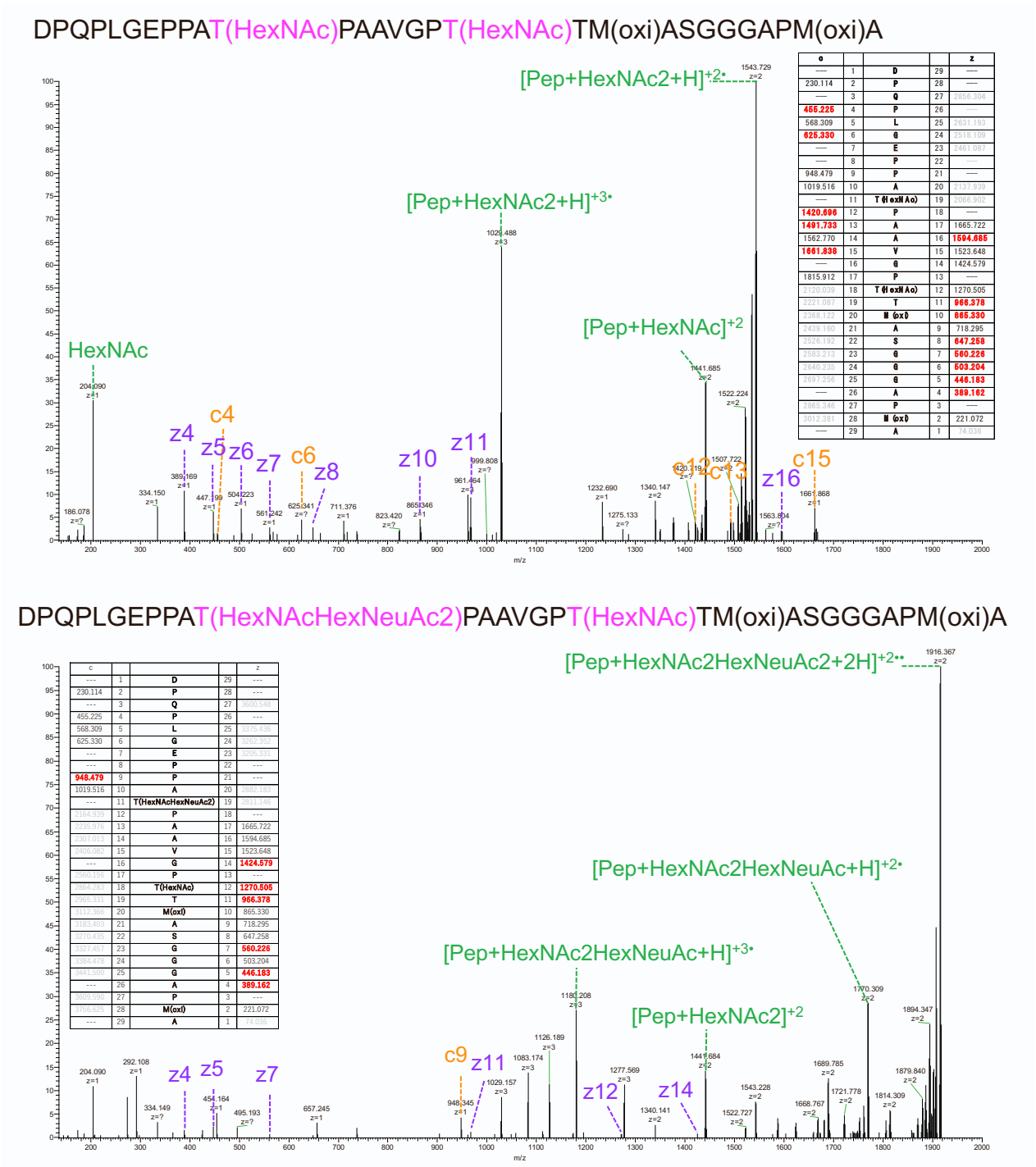

Figure S9. The EThcD mass spectra of D184–A212 modified with HexNAc at T194 and T201 (top), and HexNAcHexNeuAc2 at S194 and HexNAc at T201 (bottom).

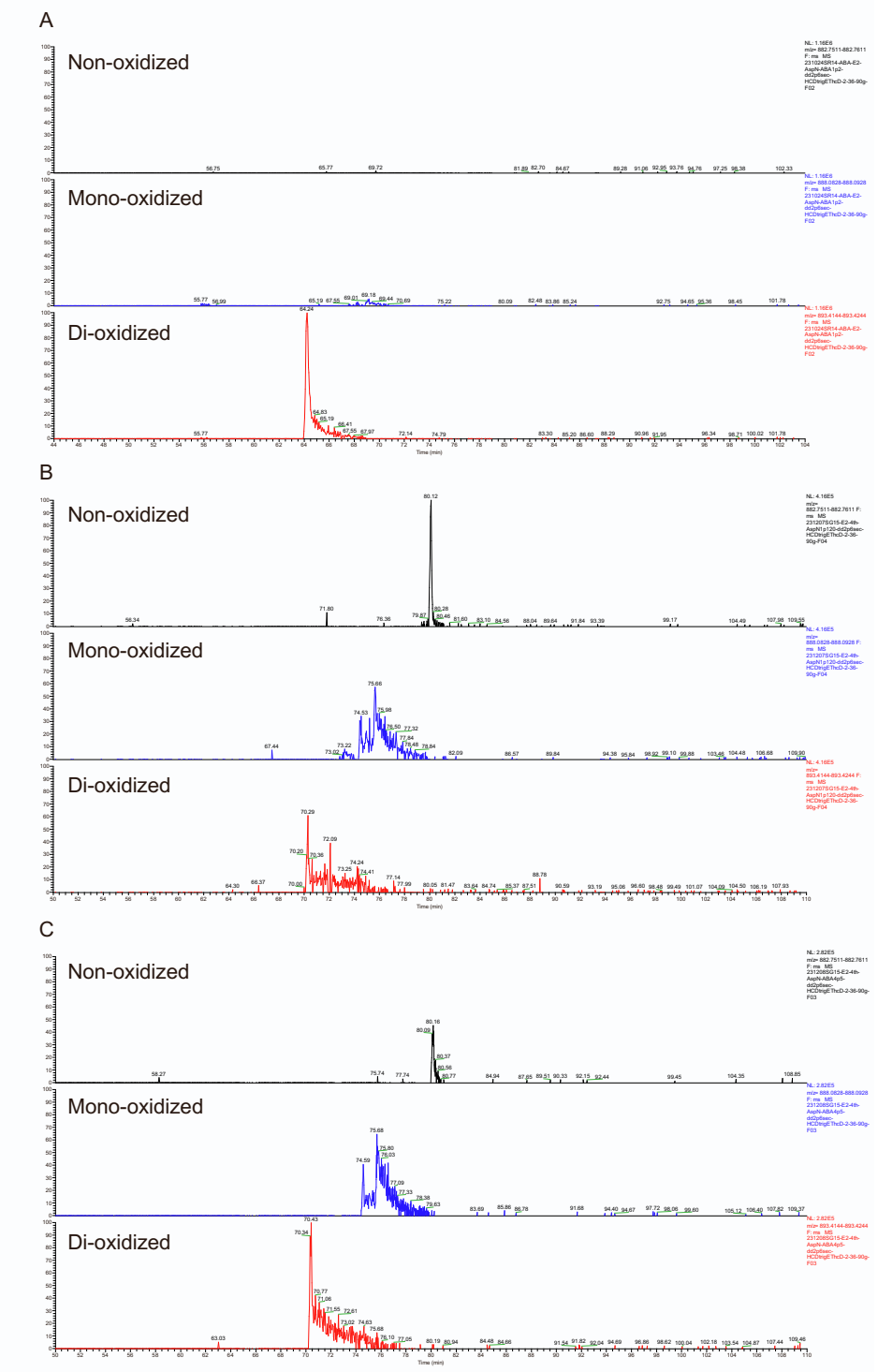

Figure S10. XICs of D184-A212 modified by non- (*m/z* 882.7561 ± 0.005; top), mono- (*m/z* 882.0878 ± 0.005; middle), and di-oxidized form (*m/z* 893.4194 ± 0.005; bottom) in (A) the ABA-bound fraction of the peptides digested from ABA-bound rAAV6 with the S-trap column, (B) the peptides digested from ABA-bound rAAV6 without the S-trap column, and (C) the peptides digested from ABA-bound rAAV6 with the S-trap column. The non-oxidized form was abundant for rAAV6 digested without the S-trap digestion, whereas the ratio of mono- and di-oxidized form to non-oxidized form increased after the S-trap digestion. We therefore suspect that some reagent used in the S-trap digestion may accelerate the oxidation of methionine.

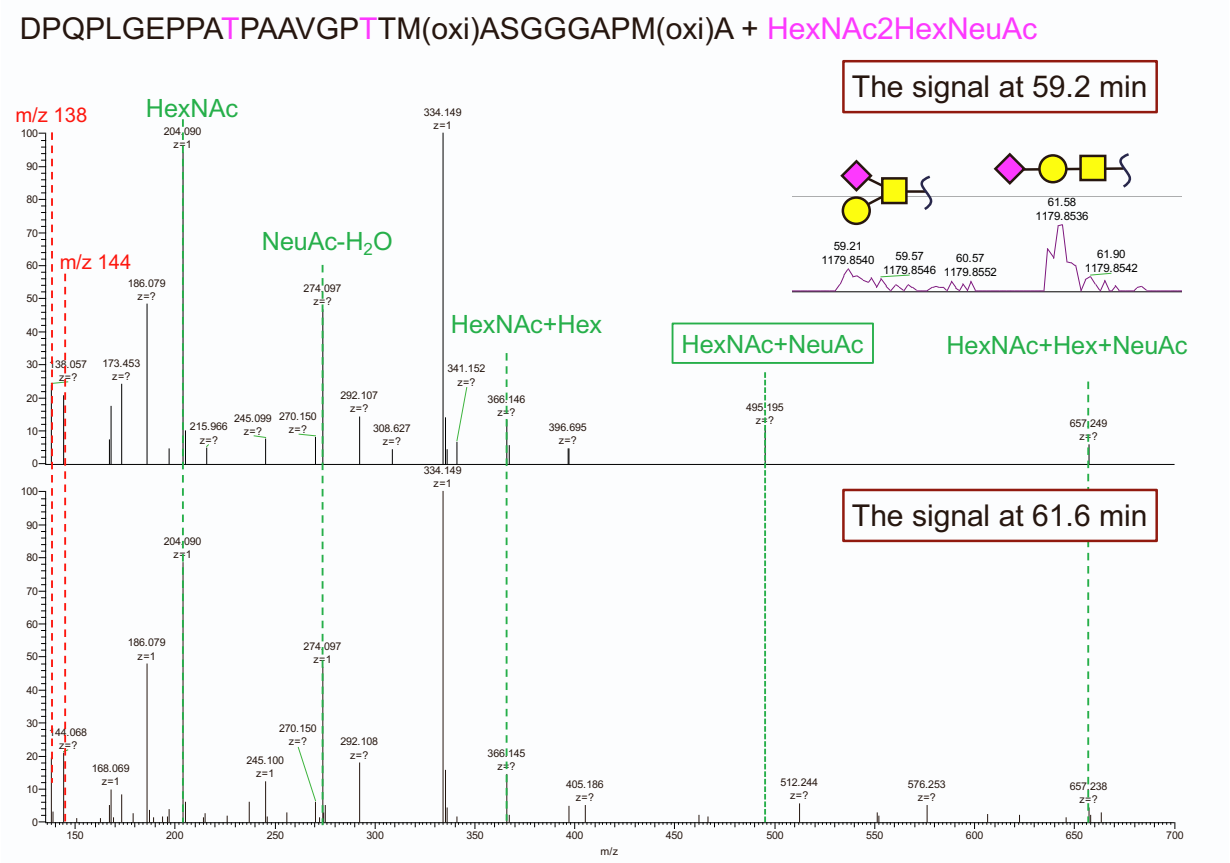

Figure S11. The HCD mass spectra of the signals at 59.2 min and 61.6 min for D184–A212 modified with HexNAc2HexNeuAc. The signals *m/z* 138 and *m/z* 144 showed similar intensities.

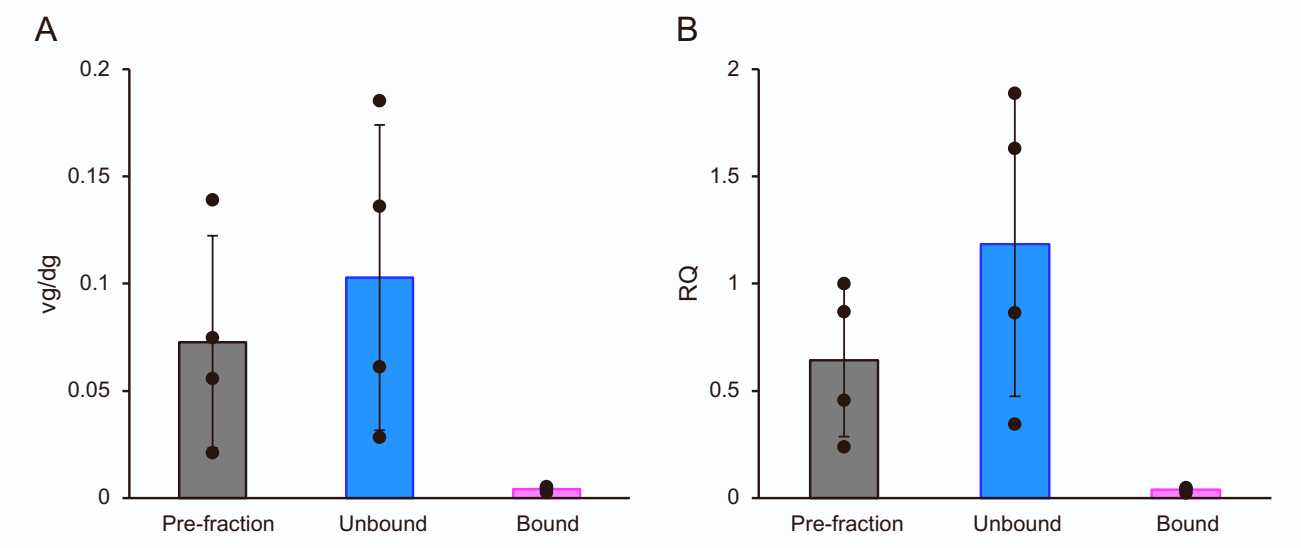

Figure S12. (A) rAAV6 genomes per mouse diploid genome (vg/dg) and (B) *hFIX* mRNA levels in liver tissue were determined using qPCR 8 weeks after rAAV6 administration. Individual points are shown in black circles, and error bars shows the SD value for n = 4.

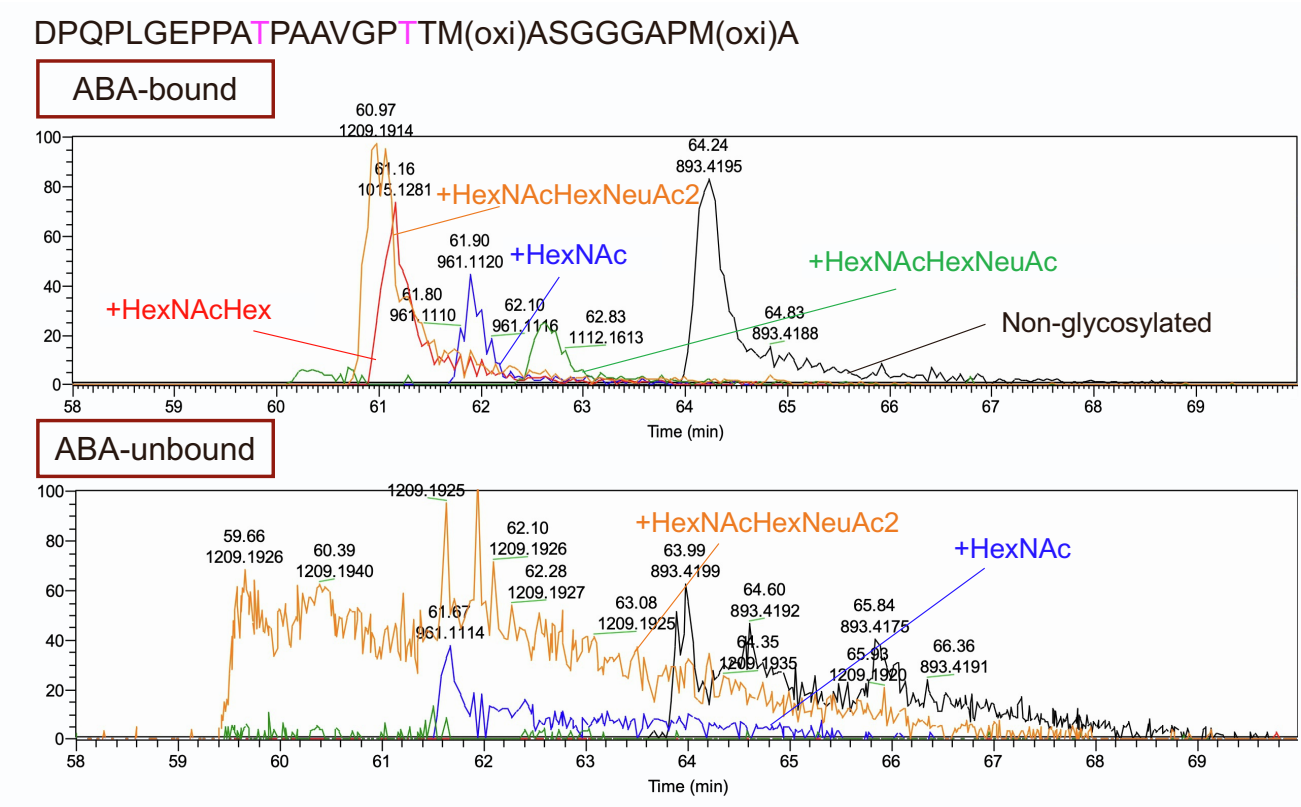

Figure S13. XICs of D184–A212 modified with mucin-type *O*-glycan clusters. The signal of non-glycosylated peptide (*m/z* 893.4194 ± 0.005) is colored black, HexNAc (*m/z* 961.1025 ± 0.005) is blue, HexNAcHex2 (*m/z* 1015.1231 ± 0.005) is red, HexNAcHexNeuAc (*m/z* 1112.1619 ± 0.005) is green, and HexNAcHexNeuAc2 (*m/z* 1209.1937 ± 0.005) is orange.